

Flavorful leptoquarks at hadron colliders

Gudrun Hiller* and Dennis Loose†

Fakultät Physik, TU Dortmund, Otto-Hahn-Str.4, D-44221 Dortmund, Germany

Ivan Nišandžić‡

Institut für Theoretische Teilchenphysik, Karlsruher Institut für Technologie, D-76128 Karlsruhe, Germany

B -physics data and flavor symmetries suggest that leptoquarks can have masses as low as few $\mathcal{O}(\text{TeV})$, predominantly decay to third generation quarks, and highlight $pp \rightarrow b\mu\mu$ signatures from single production and $pp \rightarrow bb\mu\mu$ from pair production. Abandoning flavor symmetries could allow for inverted quark hierarchies, and cause sizable $pp \rightarrow j\mu\mu$ and $jj\mu\mu$ cross sections, induced by second generation couplings. Final states with leptons other than muons including lepton flavor violation (LFV) ones can also arise. The corresponding couplings can also be probed by precision studies of the $B \rightarrow (X_s, K^*, \phi)ee$ distribution and LFV searches in B -decays. We demonstrate sensitivity in single leptoquark production for the LHC and extrapolate to the high luminosity HL-LHC. Exploration of the bulk of the phase space requires a hadron collider beyond the reach of the LHC, with b -identification capabilities.

I. INTRODUCTION

Leptoquarks generically couple differently to different generations of quarks and leptons. Present hints of non-universality between electrons and muons in the rare B -decay observables R_K, R_{K^*} [1] by the LHCb collaboration [2, 3] are indeed naturally explained by tree-level exchange of leptoquarks [4–16]. Combining R_K with R_{K^*} allows to diagnose the chirality of the participating $|\Delta b| = |\Delta s| = 1$ currents [17]. Current data favor leptoquarks that couple to quark- and lepton doublets, *e.g.*, [18–23] implying couplings to both b - and t -quarks, and charged leptons and neutrinos. The corresponding leptoquark representations are the scalar $SU(2)_L$ -triplet S_3 and two vectors, a singlet V_1 and a triplet, V_3 . Importantly, the mass scale of the leptoquarks is model-independently limited by multi- $\mathcal{O}(10)$ TeV, and in viable flavor models in the TeV-range, suggesting dedicated searches at the Large Hadron Collider (LHC) and beyond [24].

*Electronic address: ghiller@physik.uni-dortmund.de

†Electronic address: dennis.loose@udo.edu

‡Electronic address: ivan.nisandzic@kit.edu

Search results for leptoquarks are available for fixed branching fractions into a given lepton species. For instance, mass limits for leptoquarks decaying 50 % to electrons (muons) plus jet and the other 50 % to neutrinos and a jet are 900 GeV (850 GeV) [25], with similar results reported in [26, 27], all obtained from pair production. The limits improve to 1100 GeV [26] (1080 GeV [27]) for 100 % decay to electrons (muons) plus jet. Bounds from single production in jet ee (1755 GeV) and jet $\mu\mu$ (660 GeV) [28] assume 100 % decays to charged leptons and coupling equal to one. As we will show, rare B -decay data suggest to look for leptoquarks with dominant decays to $b\ell$, $\ell = e, \mu$. To date, no corresponding leptoquark search has been performed at the LHC. On the other hand, derived limits from other searches such as supersymmetry resulting in analogous signatures as the leptoquark ones are 1.5 TeV (S_3) and 1.8 TeV ($V_{1,3}$) for be , and 1.4 TeV (S_3) and 1.7 TeV ($V_{1,3}$) for $b\mu$ [29]. Limits on $b\nu, t\ell, t\nu$ are not stronger.

The aim of this study is to work out collider signatures of leptoquark scenarios that take into account flavor structure and B -physics data. We focus on single production, which is directly driven by the leptoquark couplings to quarks and leptons and results in signatures with a quark and two leptons. Flavor physics provides directions to identify the final states with leading signatures. We work out explicit predictions for the scalar leptoquark S_3 ; the flavor aspects of the analysis are analogous for the vector ones. We estimate improvements in mass reach for possible future pp -machines operating at center-of-mass energies $\sqrt{s} = 33$ TeV (HE-LHC) and 100 TeV (FCC-hh) [24, 30]. For related recent works on leptoquark production and R_{K,K^*} , see [31–33].

The paper is organized as follows: In section II we review the requirements and constraints from flavor physics on the leptoquark's mass and couplings. Leptoquark branching ratios and single as well as pair production are discussed in section III. Expectations for the flavor patterns of the leptoquark couplings are given in section IV, together with corresponding branching ratios and signal strengths. In section V we conclude.

II. THE SCALAR LEPTOQUARK S_3

We denote by S_3 the scalar leptoquark that resides in the $(\bar{3}, 3, 1/3)$ representation of the SM gauge group. Its couplings to the SM fermions are given by the following Lagrangian:

$$\mathcal{L}_{\text{Yuk}} = \lambda \bar{Q}_L^C \alpha (i\sigma^2)^{\alpha\beta} (S_3)^{\beta\gamma} L_L^\gamma + Y_\kappa \bar{Q}_L^C \alpha (i\sigma^2)^{\alpha\beta} (S_3^\dagger)^{\beta\gamma} Q_L^\gamma + \text{h.c.}, \quad (1)$$

where σ^2 is the second Pauli matrix and α, β, γ are $SU(2)_L$ indices, while ψ^C denotes the charge conjugated spinor. We concentrate in this work on the first term that involves the coupling to

leptons and quarks and assume the existence of a mechanism that forbids the second term that is potentially dangerous with regards to proton decay. Our interest is therefore focused on the Yukawa coupling matrix λ , a 3×3 matrix in flavor space with rows (columns) carrying a quark (lepton) flavor index, that we suppress for the moment to avoid clutter. The S_3 can be represented in terms of its isospin components as

$$S_3 = \begin{pmatrix} S_3^{1/3} & \sqrt{2}S_3^{4/3} \\ \sqrt{2}S_3^{-2/3} & -S_3^{1/3} \end{pmatrix}, \quad (2)$$

where the superscripts denote the electric charge in units of e . The normalization is fixed to yield canonically normalized kinetic terms for the complex scalar components.

Expanding the Lagrangian (1) in terms of the isospin components we obtain

$$\mathcal{L}_{\text{QL}} = -\sqrt{2}\lambda \bar{d}_L^C \ell_L S_3^{4/3} - \lambda \bar{d}_L^C \nu_L S_3^{1/3} + \sqrt{2}\lambda \bar{u}_L^C \nu_L S_3^{-2/3} - \lambda \bar{u}_L^C \ell_L S_3^{1/3} + \text{h.c.} \quad (3)$$

The kinetic term for the leptoquark multiplet is written as

$$\mathcal{L}_{\text{kin}} = \frac{1}{2} \text{Tr} \left[(D_\mu S_3)^\dagger D^\mu S_3 \right]. \quad (4)$$

We assume the approximate mass degeneracy of the components within the multiplet. For the collider study in section III we implement the model (3), (4) in `Feynrules` [34] to obtain the corresponding Universal Feynrules Output (`UFO`) [35]. The latter is used as input to the `MadGraph` event generator code [36].

To successfully accommodate present $R_{K^{(*)}}$ data with the S_3 one requires [21]

$$\lambda_{b\mu}\lambda_{s\mu}^* - \lambda_{be}\lambda_{se}^* \simeq 1.1 \frac{M_{S_3}^2}{(35 \text{ TeV})^2}. \quad (5)$$

Here, we label the element of the leptoquark Yukawa matrix $\lambda = \lambda_{q\ell}$ by the quark and lepton flavors it couples to. By $SU(2)_L$, $\lambda_{U_i\ell} = V_{ji}^* \lambda_{D_j\ell}$, where V denotes the CKM matrix, and $U = u, c, t$, $D = d, s, b$ and $i, j = 1, 2, 3$. Assuming $i)$ that the SM hierarchies for the quark Yukawas are intact in the leptoquark ones, couplings to third generation quarks are dominant [7, 37],

$$\lambda_{d\ell} \sim (\epsilon^3 \dots \epsilon^4) \lambda_{b\ell}, \quad \lambda_{s\ell} \sim \epsilon^2 \lambda_{b\ell}, \quad \ell = e, \mu, \tau. \quad (6)$$

This can, for instance, be realized with a Froggatt-Nielsen-Mechanism [38], where $\epsilon \sim 0.2$ denotes a flavor parameter of the size of the sine of the Cabibbo angle. The \sim symbol indicates that a relation holds up to factors of order one. Charged lepton mass hierarchies are taken care of by the $SU(2)_L$ -singlet leptons, *i.e.*, the lepton doublets are neutral under the Froggatt-Nielsen symmetry

and no further suppressions in $\lambda_{q\ell}$ appear. Taking in addition into account that *ii)* the BSM effects in R_{K,K^*} are predominantly from muons as opposed to electrons as corresponding contributions are consistent with those from global fits to the $b \rightarrow s\mu^+\mu^-$ observables [39], a viable "simplified" benchmark λ_s is obtained as

$$\lambda_s \sim \lambda_0 \begin{pmatrix} 0 & 0 & 0 \\ * & \epsilon^2 & * \\ * & 1 & * \end{pmatrix}. \quad (7)$$

Here the entries denoted by "0" are of higher order in ϵ ; they are constrained by μ - e conversion and rare kaon decays and of no concern to the present analysis. The entries labeled with an asterisk are not needed to explain $|\Delta b| = |\Delta s| = 1$ data. Eq. (5) implies $\lambda_0 \simeq M_{S_3}/6.7$ TeV. Allowing for order one factors in $\lambda_{s\mu}$, taken here to be between 1/3 and 3, one obtains the range

$$M_{S_3}/11.6 \text{ TeV} \lesssim \lambda_0 \lesssim M_{S_3}/3.9 \text{ TeV}. \quad (8)$$

The parameter space (8) is well within the LHC-limits on Drell-Yan production, to which t -channel leptoquarks contribute at tree level. Specifically, the Wilson coefficient $C_{b_L L} = v^2 \lambda_0^2 / (2M_{S_3}^2)$ satisfies in our case $C_{b_L L} \lesssim 2 \cdot 10^{-3}$, where $v = 246$ GeV denotes the vacuum expectation value (vev) of the Higgs, while experimentally it is constrained only at the level of 10^{-2} for both electrons and muons [40]. Note that the effective theory is constructed to hold for leptoquark masses greater than the dilepton invariant mass, presently up to a few TeV. However, also for smaller masses effective theory bounds provide a useful approximation [41].

III. COLLIDER SIGNATURES

We discuss leptoquark decays and single leptoquark production at proton-proton colliders in section III A and III B, respectively. In section III C we consider signatures with tops and jets. We occasionally use the symbol ϕ for a generic leptoquark.

A. Decay and width

Neglecting the masses of the decay products, the partial decay width of a scalar leptoquark S_3 with mass M decaying to a lepton ℓ and a quark q reads

$$\Gamma(S_3 \rightarrow q\ell) = c \frac{|\lambda_{q\ell}|^2}{16\pi} M, \quad (9)$$

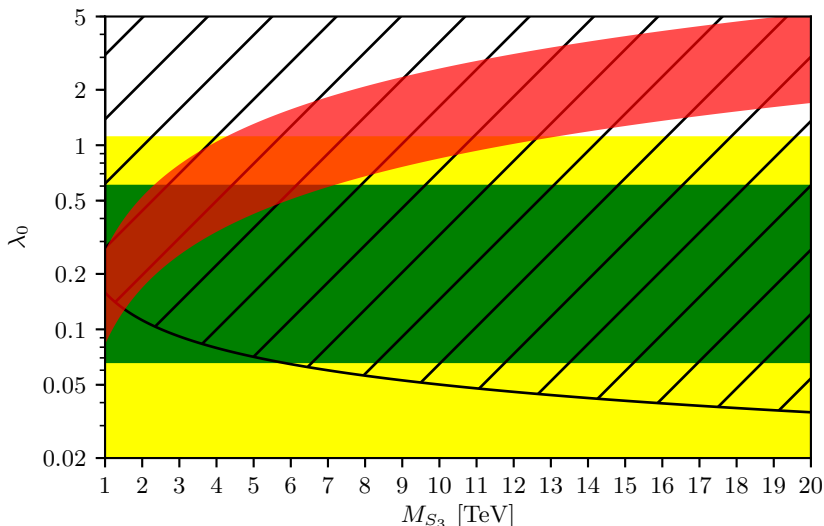


Figure 1: Leptoquark parameter space, mass M_{S_3} versus coupling, in the simplified scenario assuming a single dominant coupling λ_0 for $S_3^{4/3}$. The red band shows the range relevant to R_K, R_{K^*} -data, (8), the yellow (shaded) region refers to a narrow width $\Gamma/M_{S_3} \lesssim 5\%$, and in the hatched area above the black curve holds $\Gamma > \Lambda_{QCD}$. Flavor model predictions [16] are given by the green horizontal band. See text for details.

where $c = 2$ for $S_3^{4/3}$, $S_3^{-2/3}$ and $c = 1$ for $S_3^{1/3}$, see eq. (3). Γ approximates the total width if the coupling $\lambda_{q\ell}$ is the dominant one. Note that the multi-body decays induced by inter-multiplet cascades such as $S_3^{-4/3} \rightarrow S_3^{-1/3}W^- \rightarrow b\nu W^-$ can become sizable for large masses. With couplings to the first and second quark generation being flavor-suppressed, as, for instance, made explicit in (7) and following text, the leptoquark predominantly decays to third generation quarks. The relevant parameter space in mass and leading coupling $\lambda_0 \equiv \lambda_{b\mu}$ is illustrated in figure 1 for the $S_3^{4/3}$. The yellow (shaded) region corresponds to a narrow width, $\Gamma/M_{S_3} \lesssim 5\%$, which translates to $\lambda_0 \lesssim 1.1$. (Note, $\Gamma/M_{S_3} \lesssim 1\%$ (10%) corresponds to $\lambda_0 \lesssim 0.5$ (1.6).) The red band denotes the region that explains lepton non-universality (LNU)-data, (8). In the hatched region above the black curve the leptoquark decays too rapid to form bound states, $\Gamma > \Lambda_{QCD}$. Predictions from viable flavor models $\lambda_{b\mu} \sim c_\ell$, where c_ℓ is of the order ϵ [16] (green horizontal band) are also shown. B_s -mixing data together with R_K, R_{K^*} provide a data-driven upper limit on the mass of the S_3 leptoquark of 40 TeV. For such large masses the coupling required by B -physics data becomes order one and approaches the perturbativity limit. In addition, the region of narrow width is left. Upper mass limits on the (gauge-like) vector leptoquarks are 45 TeV and 20 TeV for V_1 and V_3 , respectively [21]¹.

¹ Recent analysis of B_s -mixing [42] suggests lower upper limits on the leptoquark masses.

We list the dominant decays modes for the three leptoquark representations that can explain current LNU-data [21], for the scalar isospin triplet

$$\begin{aligned}
S_3^{+2/3} &\rightarrow t \nu, \\
S_3^{-1/3} &\rightarrow b \nu, t \mu^-, \\
S_3^{-4/3} &\rightarrow b \mu^-,
\end{aligned}
\tag{10}$$

the vector isospin singlet

$$V_1^{+2/3} \rightarrow b \mu^+, t \nu \tag{11}$$

and the vector isospin triplet

$$\begin{aligned}
V_3^{-1/3} &\rightarrow b \nu, \\
V_3^{+2/3} &\rightarrow b \mu^+, t \nu, \\
V_3^{+5/3} &\rightarrow t \mu^+.
\end{aligned}
\tag{12}$$

As, for instance, $V_1^{-2/3} \rightarrow \bar{b} \mu^-$ and $S_3^{-4/3} \rightarrow b \mu^-$ lead both to a negatively charged lepton, tagging of the b -charge would be useful to identify the leptoquark type and its electric charge.

Note that some leptoquarks can undergo more than one decay into the third generations quarks, such as $S_3^{-1/3}$, (10) and in this case, by $SU(2)_L$, $\mathcal{B}(\phi \rightarrow b\nu_\ell) \sim \mathcal{B}(\phi \rightarrow t\ell) \simeq 1/2$. Similarly, for V_1 (11) and V_3 (12), $\mathcal{B}(\phi \rightarrow b\ell) \sim \mathcal{B}(\phi \rightarrow t\nu_\ell) \simeq 1/2$.

B. Single leptoquark production

In figure 2 we show the leading order diagrams inducing single leptoquark production, followed by its decay. The production is in association with a lepton. The cross section is sensitive to the flavor coupling $\lambda_{q\ell}$. With the couplings to the first and second quark generations being flavor-suppressed, the parton level production of the leptoquark is dominated by the third generation coupling. This continues to be the case at hadron level, which can be inferred from figure 3. The parton distribution function (PDF) suppression of b -production (dotted blue curve) versus s -production (dashed-dotted orange curve) is about a factor of $(\text{few})^{-1}$ and the one of b -production versus d -production (dashed pink curve) is of the order 10^{-1} to 10^{-2} , which are weaker than the respective flavor suppressions (6), so indeed, beauty wins. In figure 3 we added the cross sections of CP-conjugate final states; in the absence of CP-violation, which is the limit we are working in, this amounts to a factor 2 in the

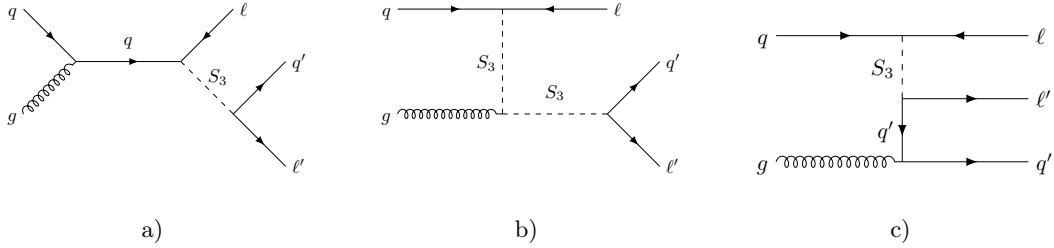


Figure 2: Leading order diagrams for single leptoquark production and decay: Diagrams a), b) correspond to resonant amplitudes. Diagram c) corresponds to a non-resonant contribution, the effects of which are suppressed through kinematic cuts, see section III B for details.

single production cross section from valence quark-gluon fusion. Also shown in the two additional plots are predictions for future proton-proton machines, a 33 TeV HE-LHC and a 100 TeV collider.

The corresponding numerical calculations are performed using **Madgraph v.2.6** [36] at leading order in QCD. We find that the largest uncertainties originate from the PDFs (we use LHAPDF [43]). For the single production (red band) linked to $R_{K^{(*)}}$ -data (8) they grow from order ten percent for $M \sim 1$ TeV to $\sim 35 - 40$ percent for smaller cross sections of $\text{few} \times 10^{-7}$ pb. The scale uncertainty – in our estimate both the factorization and the renormalization scale are equal to half of the sum of the transverse masses of the final state particles – reaches ~ 25 percent.

In figure 3 the cross section for pair production $\sigma(pp \rightarrow S_3^{-4/3} S_3^{+4/3})$ is shown by the solid green curve. We find, using Madgraph at leading order, that both PDF and scale uncertainties can reach $\mathcal{O}(40)$ percent towards $\sigma \sim \text{few} \times 10^{-7}$ pb. While the scale uncertainty is essentially flat the PDF uncertainty drops to order 10 percent for lighter leptoquarks near a TeV. In the simplified benchmark (7) the $S_3^{\pm 4/3}$ decays into $b\mu$, see (10), producing a $pp \rightarrow bb\mu\mu$ signature. Pair production of another component of the S_3 can give $tt\mu\mu$, bbE_{miss} , $bt\mu E_{\text{miss}}$ or ttE_{miss} final states.

For low masses, pair production has a larger cross section than single production (red band) linked to $R_{K^{(*)}}$ -data (8), while the single production cross section is larger for higher masses. Naively, about a factor ~ 2 (5) in mass reach can be gained in pair production at a 33 (100) TeV collider relative to 13 TeV and for comparable luminosity of 3000 fb^{-1} . The potential gain for single production is somewhat larger: about a factor ~ 2.5 (7) in the target parameter space - the red band - for 33 (100) TeV. While this gives an idea about the accessible ranges dedicated simulations are needed to estimate the reach more reliably.

We simulate events for a 1.5 TeV leptoquark and different couplings at the $\sqrt{s} = 13$ TeV LHC. In figure 4 we present the corresponding distributions for signal and background as a function of

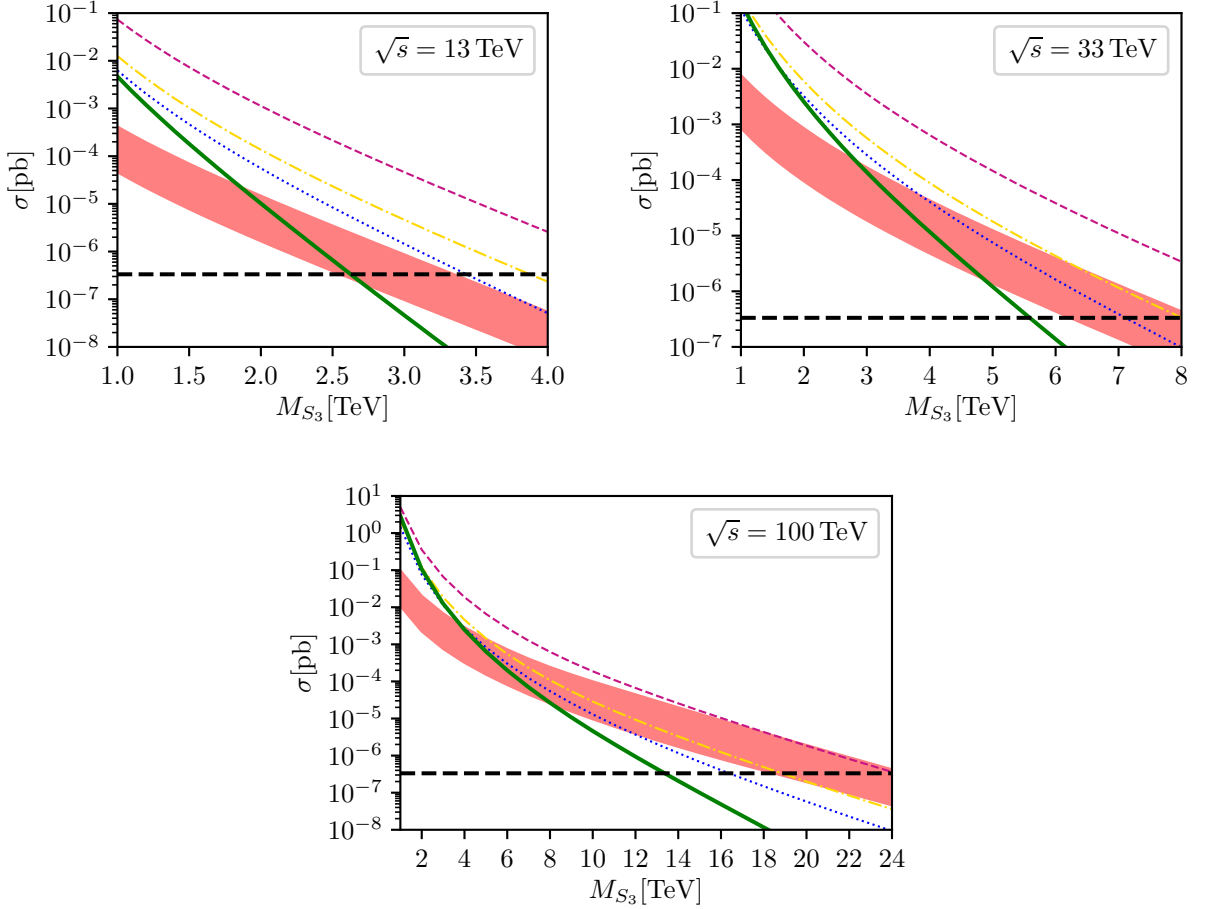


Figure 3: The single leptoquark production cross section $\sigma(pp \rightarrow S_3^{-4/3} \mu^+ + S_3^{+4/3} \mu^-)$ as a function of the mass M_{S_3} for $\sqrt{s} = 13, 33$ and 100 TeV. The red band corresponds to the flavor pattern (7) with λ_0 in accord with the B -anomalies (8). The triplet of (thin) curves illustrates the single production cross section with one coupling switched on at a time (from top to bottom: dashed pink, dashed-dotted orange and dotted blue for $\lambda_{d\mu, s\mu, b\mu}$ set to one, respectively). The pair production cross section $\sigma(pp \rightarrow S_3^{-4/3} S_3^{+4/3})$ is shown by the green (thick, solid) curve. The black (dashed) line corresponds to the absolute lower limit of the cross section below which one cannot produce a single event with integrated luminosity 3000 fb^{-1} . See text for details.

$M_{\text{inv}}(\mu^-, b)$, the invariant mass of the μ^-b -system. To enhance the significance and to study a situation where the b -charge is not tagged, we add the CP-conjugate process $pp \rightarrow \bar{b}\mu^+\mu^-$ in both signal and background. The corresponding calculations are performed at leading order in QCD using `Madgraph v.2.6` [36] for the event generation, `PYTHIA 8` [44] for the parton showering and hadronization and `DELPHES 3` [45] for the fast detector simulation. For the muon isolation we follow [28], while all the other criteria are taken from the default Delphes card for the CMS

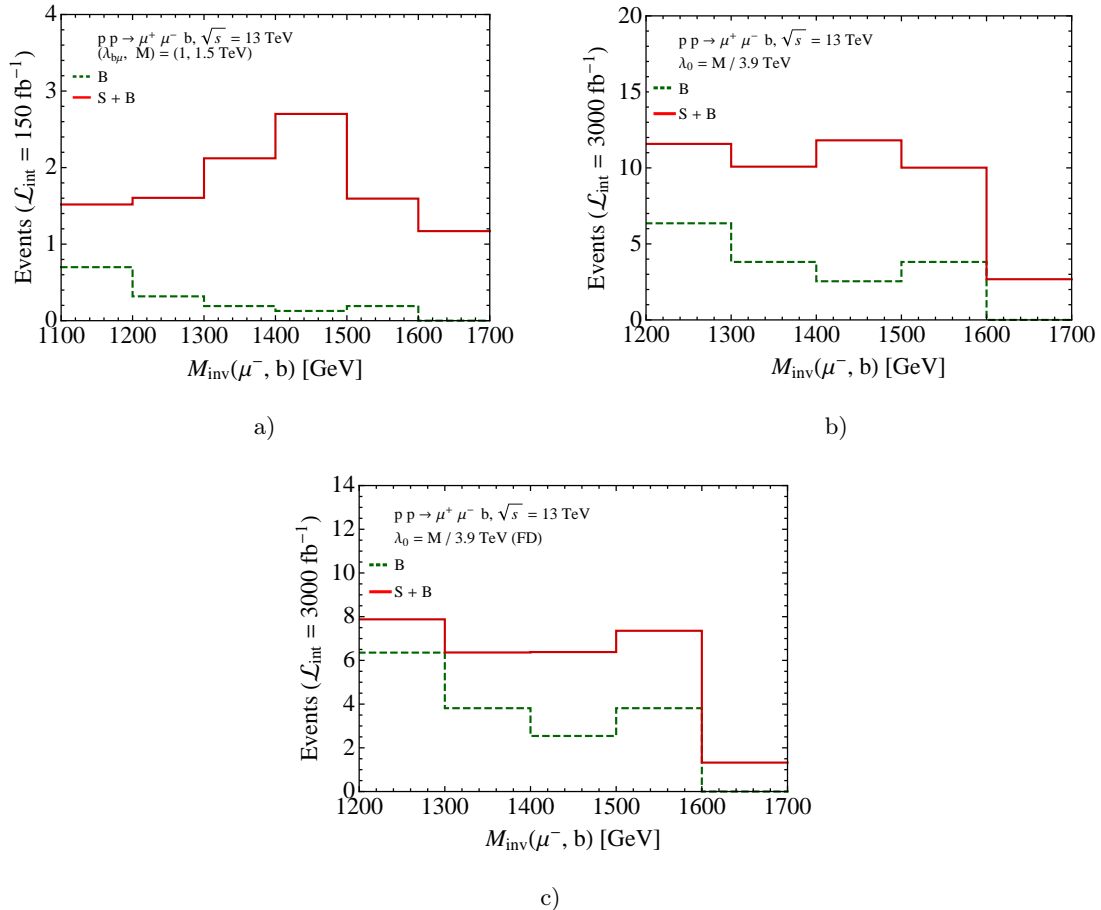


Figure 4: Distribution of events over the invariant mass of the μ^- - b -jet system from $pp \rightarrow b\mu^+\mu^-$ and $pp \rightarrow \bar{b}\mu^+\mu^-$ at $\sqrt{s} = 13$ TeV. All three plots correspond to a leptoquark with mass 1.5 TeV. a) corresponds to $\lambda_{b\mu} = 1$, and b) to the flavor pattern (7) with $\lambda_0 = M/3.9$ TeV in accord with B -anomalies (8). The pattern (15) on which c) is based similarly addresses B -data but allows additionally for decays to taus. The dashed green (solid red) line represents background (signal and background) events. Kinematic cuts are described in the text.

detector. To account for the QCD corrections at NLO we multiply signals and backgrounds with corresponding global k -factors. For the signal we use $k \sim 1.5$ [46], while for the background we use the value that we obtain from comparing the NLO and LO calculations at fixed order in Madgraph. For the analysis of the signal and background we use `MadAnalysis 5` [47].

For these evaluations we adopt the following kinematic cuts: We accept events containing two opposite charge muons and a b -jet and require for the transverse momenta and absolute pseudorapidities of each of these final states to exceed 45 GeV and to be smaller than 2.1, respectively. Furthermore, for the angular separation between muon and a b -jet we have $\Delta R > 0.3$ and also we

cut on the invariant mass of the opposite-charge muon-pair $M_{\text{inv}} > 110 \text{ GeV}$. For the final event selection we adopt the cut on the scalar sum of the transverse momenta of muon-pair and leading b -jet $S_T(\mu_1, \mu_2, b_1) > 250 \text{ GeV}$ [28]. We use $M_{\text{inv}}(\mu, b\text{-jet})$ as a discriminating variable between signal and background and adjust the corresponding cut to a given mass and coupling hypothesis in order to maximize the significance of the signal.

The approximate expected discovery significance for the first case (a) $\lambda_{b\mu} = 1$, which is a priori unrelated to LNU-data, is around 4σ for an integrated luminosity of 150 fb^{-1} . In the second case (b) where $\lambda_{b\mu}$ saturates the upper limit in (7),(8) we find around 5σ at 3000 fb^{-1} . The significance for the third case c) is smaller, somewhat below 3σ due to the twice smaller branching fraction into $b\mu$, see (15). To compute these significances we used the approximate formula from [48] and took into account both μ^-b^- and $\mu^+\bar{b}^-$ signals in the data sample.

C. Tops and jets

We briefly discuss single production into top and jet plus dilepton final states, which complements searches into b 's.

The processes $gb \rightarrow \mu^+\phi(\rightarrow b\mu^-)$ are related to $gb \rightarrow \nu\phi(\rightarrow t\mu^-)$ by $SU(2)_L$, and arise at the same order of flavor counting. We recall the factor $1/2$ in the leading $S_3^{-1/3}$ branching ratios as within our approximations the leptoquark decays to both $b\nu$ and $t\ell$ via λ_0 at equal rate. However, the $t\mu\nu$ final state has larger background because SM processes from $W \rightarrow \ell\nu$ cannot be removed equally well as $Z \rightarrow \ell\ell$. On the other hand, if the flavor suppression of the second generation quark coupling is not realized in nature, $t\mu\mu$ final states, induced by $\lambda_{c\mu} \simeq \lambda_{s\mu}$, could potentially be interesting. For $\lambda_{b\mu} = \lambda_{s\mu}$ one finds for the branching ratio $\mathcal{B}(\phi \rightarrow t\mu) \simeq 1/4$, however, the leptoquark coupling drops by an order of magnitude, $\lambda_0 = 0.03M/\text{TeV}$, as dictated by (5). Despite the PDF enhancement from charm relative to b this democratic scenario results in about two orders of magnitude smaller cross sections relative to $pp \rightarrow b\mu\mu$.

Inverted hierarchies $\lambda_{s\mu} \gg \lambda_{b\mu}$ are in conflict with flavor symmetry, see section IV, but not excluded experimentally in the simplified scenario with two entries only (7). This extreme scenario however does not improve the situation regarding $t\mu\mu$, as the branching ratio into $t\mu$ is suppressed as $|\lambda_{b\mu}/\lambda_{s\mu}|^2$ while the product of couplings is fixed by B -data (5). On the other hand, jet plus dileptons benefits from the large second generation Yukawa while having an order one branching ratio. Note that jet plus charged lepton final states can arise from several components of the $SU(2)_L$ -multiplets (10)-(12). Using the upper limit $\lambda_{s\mu} \lesssim M/2 \text{ TeV}$ from Drell-Yan production at

the LHC [40] and taking into account the PDF enhancement second quark generation cross sections $\sigma(pp \rightarrow (j\mu^-)\mu^+ + (j\mu^+)\mu^-)$ can be about an order of magnitude larger than the maximum third generation ones in accord with B -anomalies (8), shown by the red band in figure 3. A detailed analysis of the sensitivity to inverted hierarchies including reconstruction efficiencies is left for future work.

IV. FLAVOR BENCHMARKS

We explain how the simplified pattern (7) can arise in models of flavor and give more general Yukawa patterns. We are in particular interested in theoretical predictions for the entries with an asterisk, that potentially induce leptoquark signals with electrons or taus, and LFV, which affects the collider phenomenology.

The most general approach, treating all entries as free parameters only constrained by upper limits and (5), presently does not suffice to identify the dominant collider signatures. We therefore suggest to study benchmarks. They are motivated by viable flavor symmetries that successfully explain SM flavor, and consistency with data.

A simultaneous explanation of the LNU-ratios R_K, R_{K^*} and $B \rightarrow K^*\mu^+\mu^-$ angular distributions is possible with BSM effects in couplings to muons alone. Hence, from this perspective, leptoquark couplings to electrons are *not necessary*. Lepton species isolation patterns can be engineered with discrete, non-abelian flavor symmetries such as A_4 [7]. For second generation leptons, these read

$$\lambda_\mu \sim c_\ell \begin{pmatrix} 0 & \epsilon^4 & 0 \\ 0 & \epsilon^2 & 0 \\ 0 & 1 & 0 \end{pmatrix} \rightarrow c_\ell \begin{pmatrix} \delta\epsilon^4 & \epsilon^4 & \delta\epsilon^4 \\ \delta\epsilon^2 & \epsilon^2 & \delta\epsilon^2 \\ \delta & 1 & \delta \end{pmatrix} \quad (13)$$

or, one that avoids the CKM suppression for the second generation quarks [16],

$$\tilde{\lambda}_\mu \sim \begin{pmatrix} 0 & c_\ell\epsilon^4 & 0 \\ c_\nu\kappa & c_\nu\kappa & c_\nu\kappa \\ 0 & c_\ell & 0 \end{pmatrix} \rightarrow \begin{pmatrix} c_\nu\kappa\epsilon^2 & c_\ell\epsilon^4 + c_\nu\kappa\epsilon^2 & c_\nu\kappa\epsilon^2 \\ c_\nu\kappa & c_\ell\epsilon^2 + c_\nu\kappa & c_\nu\kappa \\ c_\ell\delta + c_\nu\kappa\epsilon^2 & c_\ell & c_\ell\delta + c_\nu\kappa\epsilon^2 \end{pmatrix}. \quad (14)$$

In (13) and (14) all vevs c_ℓ, c_ν, κ are of the order ϵ^n , $n \geq 1$. δ is a small parameter of second order in the vevs, see [16] for details.

Patterns (13) and (14) receive corrections from rotating flavor to mass basis and from higher order spurion insertions [16], both of which are incorporated in the matrices to the right of the arrow. As a result, in addition to those to muons, leptoquarks couple to all leptons and third generation quarks, and LFV arises.

	$b\mu$	be	$b\tau$	$j\mu$	je	$j\tau$
λ_μ	1	δ^2	δ^2	ϵ^4	$\epsilon^4\delta^2$	$\epsilon^4\delta^2$
$\tilde{\lambda}_\mu$	1	δ^2	δ^2	$(c_\nu\kappa/c_\ell)^2$	$(c_\nu\kappa/c_\ell)^2$	$(c_\nu\kappa/c_\ell)^2$
λ_{FD}	1/2	$\kappa_e^2/2$	1/2	$\rho^2/2$	$\rho^2\kappa_e^2/2$	$\rho^2/2$

Table I: Branching fractions of leptoquark $S_3^{-4/3}$ decaying to $b\ell$ and $j\ell$, $\ell = e, \mu, \tau$ for different flavor benchmarks (13), (14) and (15), see text for details. Corresponding branching fractions of the $S_3^{-1/3}$ satisfy $\mathcal{B}(S_3^{-1/3} \rightarrow t\ell), \mathcal{B}(S_3^{-1/3} \rightarrow b\nu) \sim \mathcal{B}(S_3^{-4/3} \rightarrow b\ell)/2$ and for jets $\mathcal{B}(S_3^{-1/3} \rightarrow j\ell), \mathcal{B}(S_3^{-1/3} \rightarrow j\nu) \sim \mathcal{B}(S_3^{-4/3} \rightarrow j\ell)/2$.

For the third benchmark we employ a more general parametrization and impose experimental constraints [7] "flavor data"

$$\lambda_{\text{FD}} = \lambda_0 \begin{pmatrix} \rho_d\kappa_e & \rho_d & \rho_d\kappa_\tau \\ \rho\kappa_e & \rho & \rho\kappa_\tau \\ \kappa_e & 1 & \kappa_\tau \end{pmatrix}, \quad \kappa_\tau \sim 1. \quad (15)$$

Here we allow for quark flavor suppressions $\rho_d = \lambda_{d\ell}/\lambda_{b\ell}$ and $\rho = \lambda_{s\ell}/\lambda_{b\ell}$, with larger couplings for higher generations, in concordance with the observed quark mass pattern. In addition a suppression factor κ_e for the electrons is accounted for. The phenomenologically viable range for λ_{FD} parameters in Eq. (15) is [7]

$$\rho_d \lesssim 0.02, \quad \kappa_e \lesssim 0.5, \quad 10^{-4} \lesssim \rho \lesssim 1, \quad \kappa_e/\rho \lesssim 0.5, \quad \rho_d/\rho \lesssim 1.6. \quad (16)$$

The MEG experiment [49] can put a limit on κ_e/ρ at the level of 0.2 in the future [7].

Branching fractions of S_3 to $b\ell$ and $j\ell$, $\ell = e, \mu, \tau$ in the three benchmarks are presented in table I. They are also useful to estimate signatures in leptoquark pair production. Predictions for the vector leptoquarks follow analogous flavor patterns: Modulo the slightly different vevs [16] in $\tilde{\lambda}_\mu$ one obtains in addition $\mathcal{B}(V_1 \rightarrow b\ell) \sim \mathcal{B}(S_3^{-4/3} \rightarrow b\ell)/2$ for similar masses. In table II we give the parametric signal strength for single leptoquark production using the narrow-width approximation

$$\sigma(pp \rightarrow \phi(\rightarrow q\ell)\ell) = \sigma(pp \rightarrow \phi\ell)\mathcal{B}(\phi \rightarrow q\ell) \quad (17)$$

in the benchmarks for different final state flavors. In both tables I and II we give the leading terms in the vev expansion, $c_\ell, c_\nu, \kappa < 1$, and the flavor factors $\rho, \rho_d, \kappa_e < 1$.

Hierarchies in λ_μ and $\tilde{\lambda}_\mu$ are identical for all b -final states, but the jet² signals are less suppressed in $\tilde{\lambda}_\mu$. bee and jee channels are strongly suppressed in both benchmarks (13) and (14). For λ_{FD} the

² We use 'jet' for an object from gluons, u, d, s and c -quarks and anti-quarks, as opposed to a b -jet, made out of b and \bar{b} .

	$b\mu\mu$	$be\mu$	$b\tau\mu$	bee	$be\tau$	$b\tau\tau$	$j\mu\mu$	$je\mu$	$j\tau\mu$	jee	$je\tau$	$j\tau\tau$
λ_μ	c_ℓ^2	$c_\ell^2\delta^2$	$c_\ell^2\delta^2$	$c_\ell^2\delta^4$	$c_\ell^2\delta^4$	$c_\ell^2\delta^4$	$c_\ell^2\epsilon^4$	$c_\ell^2\delta^2\epsilon^4$	$c_\ell^2\delta^2\epsilon^4$	$c_\ell^2\delta^4\epsilon^4$	$c_\ell^2\delta^4\epsilon^4$	$c_\ell^2\delta^4\epsilon^4$
$\tilde{\lambda}_\mu$	c_ℓ^2	$c_\ell^2\delta^2$	$c_\ell^2\delta^2$	$c_\ell^2\delta^4$	$c_\ell^2\delta^4$	$c_\ell^2\delta^4$	$(c_\nu\kappa)^2$	$(c_\nu\kappa)^2$	$(c_\nu\kappa)^2$	$(c_\nu\kappa\delta)^2$	$(c_\nu\kappa\delta)^2$	$(c_\nu\kappa\delta)^2$
λ_{FD}	$\lambda_0^2/2$	$\lambda_0^2\kappa_e^2/2$	$\lambda_0^2/2$	$\lambda_0^2\kappa_e^4/2$	$\lambda_0^2\kappa_e^2/2$	$\lambda_0^2/2$	$\lambda_0^2\rho^2/2$	$\lambda_0^2\rho^2\kappa_e^2/2$	$\lambda_0^2\rho^2/2$	$\lambda_0^2\rho^2\kappa_e^4/2$	$\lambda_0^2\rho^2\kappa_e^2/2$	$\lambda_0^2\rho^2/2$

Table II: Parametric signal strength of $pp \rightarrow b\ell\ell'$ and $pp \rightarrow j\ell\ell'$ final states from single leptoquark $S_3^{-4/3}$ production for different flavor benchmarks (13), (14) and (15), see text for details.

situation depends on how strong flavor suppressions are. A small ρ implies a suppressed κ_e , (16).

We identify two limits:

A) ρ, κ_e are order one, then either λ_0 has to be small, or, if λ_0 is order one as well, then leptoquark masses are in the multi-10 TeV range. In either case there is no leptoquark-induced $b\mu\mu$ signal at the LHC.

B) $\rho, \kappa_e \ll 1$, then λ_0 is sizable, while leptoquark masses can be TeV-ish, and the jet and electron modes are suppressed.

Case B) resembles the situation for benchmarks λ_μ and $\tilde{\lambda}_\mu$. Constraints on κ_e are therefore important to control final states with electrons. For $\kappa_e \ll 1$ the ee or $e\mu$ modes would be SM-like. κ_e can be constrained from $b \rightarrow see$ or $b \rightarrow se\mu$ processes together with $b \rightarrow s\mu\mu$. Due to reduced uncertainties angular observables in $B \rightarrow K^*(\rightarrow K\pi)ee$ decays are promising [17].

In the presence of sizable couplings to more than one lepton species, such as muons and taus there are two main aspects to single production: Firstly, the signal in $pp \rightarrow (\phi \rightarrow b\mu)\mu$ drops because the leptoquark has also a decay rate into $b\tau$. This happens in plot c) of figure 4. Secondly, LFV arises, such as $pp \rightarrow (\phi \rightarrow b\tau)\mu$ and $pp \rightarrow (\phi \rightarrow b\mu)\tau$. This can be searched for in a complementary way in $B \rightarrow K^{(*)}\tau\mu$ decays.

Up to cuts and detection efficiencies, S_3 -induced $pp \rightarrow t\mu\mu$, which arises from charm quarks, see figure 2, is suppressed by ϵ^4 , $(c_\nu\kappa/c_\ell)^2$ and ρ^2 in scenario λ_μ , $\tilde{\lambda}_\mu$ and λ_{fd} , respectively, with respect to $pp \rightarrow b\mu\mu$. Using the same approximations, the $pp \rightarrow t\mu\nu$ and $pp \rightarrow b\nu\nu$ signal strength is the same as for $pp \rightarrow b\mu\mu$.

Both $S_3^{-4/3}$ and $S_3^{-1/3}$ produce $j\ell\ell'$ final states (10), hence the parametric signal strength of all jet modes in table II is additionally enhanced by a factor $\sim 3/2$. Here we used that the strange and charm PDFs are similar in size within our approximations.

V. CONCLUSION

TeV-mass leptoquarks can be singly produced at hadron colliders in association with a lepton. B -physics data, which hint at a BSM contribution in $b \rightarrow s\mu\mu$ processes, while one in $b \rightarrow see$ may be discarded by Occam's razor, together with flavor model building identify $pp \rightarrow \phi\mu \rightarrow b\mu\mu$, and two modes with missing energy $pp \rightarrow \phi\nu \rightarrow b\nu\nu$ and $pp \rightarrow \phi\nu \rightarrow t\mu\nu$, as the channels with leading cross sections. While this highlights $b\mu\mu$ as a prime channel, signatures with further final states can also be sizable and should be explored. The reasons are, firstly, to advance our understanding of flavor by probing lepton and quark flavor specific couplings in the leptoquarks' Yukawa matrix, as opposed to rare decays (5), which constrain products of couplings. Secondly, exploration of further single production modes serves as cross check with other measurements, such as leptoquark pair production and indirect searches, notably Drell-Yan production and semileptonic rare b -decays.

Due to the higher cross section for lower masses, see figure 3, we encourage searches for leptoquarks from pair production decaying to a b -quark and a lepton, or a top quark and a lepton, as in (10)-(12).

Semileptonic b -decays can be probed at LHCb and Belle II, and allow to access lepton specific couplings of all three generations, which could improve benchmarks (15) and aid collider searches. Corresponding processes are $b \rightarrow see$ and LFV, $b \rightarrow se\mu$ and those into taus. Studies of the angular distribution in $B \rightarrow K^*ee$ similar to $B \rightarrow K^*\mu\mu$ [17, 50] and searches for $B \rightarrow K^{(*)}e(\mu, \tau)$ and $B \rightarrow K^{(*)}\mu\tau$ at the level of 10^{-8} and lower, and $B_s \rightarrow e\mu$ at $\mathcal{O}(10^{-11})$ [7] should be pursued to obtain meaningful constraints on the leptoquark flavor matrix.

Discrimination between different quark flavors can be achieved by comparing signatures induced by the third generation quark coupling to the ones induced by first two generations, such as $b\ell\ell$ to $j\ell\ell$, respectively. Flavor symmetries predict the latter to be suppressed or at least not enhanced relative to the former, as a result of the corresponding quark hierarchies, *e.g.*, see patterns (13), (14) and (15). An experimental search could put this prediction to a test. Evidence for an inverted quark hierarchy $\lambda_{s\ell} \gg \lambda_{b\ell}$ would suggest an origin of flavor outside of symmetries, such as anarchy. Corresponding final states from pair production are $jj\ell\ell'$, where lepton species ℓ, ℓ' can be the same or different.

Our analysis shows that the LHC, even with 3ab^{-1} is not able to cover the full targeted parameter space, see figure 3, where also expectations for future pp -colliders with higher center of mass-energy and comparable luminosity are shown. For measurements to be useful for flavor b -identification is required. Additionally, ability to tag the flavor of the b would allow to measure the leptoquark's electric charge and distinguish leptoquark representations.

Note added: During the finalization of this work a related study on leptoquark production at colliders appeared [51].

VI. ACKNOWLEDGEMENTS

We are happy to thank Ulrik Egede, Yossi Nir and José Zurita for useful discussions. This project is supported in part by the Bundesministerium für Bildung und Forschung (BMBF).

-
- [1] G. Hiller and F. Krüger, Phys. Rev. D **69** (2004) 074020 [hep-ph/0310219].
 - [2] R. Aaij *et al.* [LHCb Collaboration], Phys. Rev. Lett. **113** (2014) 151601 [arXiv:1406.6482 [hep-ex]].
 - [3] R. Aaij *et al.* [LHCb Collaboration], JHEP **1708**, 055 (2017) [arXiv:1705.05802 [hep-ex]].
 - [4] G. Hiller and M. Schmaltz, Phys. Rev. D **90** (2014) 054014 [arXiv:1408.1627 [hep-ph]].
 - [5] B. Gripaios, M. Nardecchia and S. A. Renner, JHEP **1505** (2015) 006 [arXiv:1412.1791 [hep-ph]].
 - [6] R. Barbieri, G. Isidori, A. Pattori and F. Senia, Eur. Phys. J. C **76**, no. 2, 67 (2016) [arXiv:1512.01560 [hep-ph]].
 - [7] I. de Medeiros Varzielas and G. Hiller, JHEP **1506** (2015) 072 [arXiv:1503.01084 [hep-ph]].
 - [8] I. Doršner, S. Fajfer, A. Greljo, J. F. Kamenik and N. Košnik, Phys. Rept. **641** (2016) 1 [arXiv:1603.04993 [hep-ph]].
 - [9] S. Fajfer and N. Košnik, Phys. Lett. B **755** (2016) 270 [arXiv:1511.06024 [hep-ph]].
 - [10] D. Bečirević, N. Košnik, O. Sumensari and R. Zukanovich Funchal, JHEP **1611** (2016) 035 [arXiv:1608.07583 [hep-ph]].
 - [11] R. Alonso, B. Grinstein and J. Martin Camalich, JHEP **1510** (2015) 184 [arXiv:1505.05164 [hep-ph]].
 - [12] L. Calibbi, A. Crivellin and T. Ota, Phys. Rev. Lett. **115** (2015) 181801 [arXiv:1506.02661 [hep-ph]].
 - [13] S. Sahoo and R. Mohanta, Phys. Rev. D **91**, no. 9, 094019 (2015) [arXiv:1501.05193 [hep-ph]].
 - [14] D. Bečirević, S. Fajfer and N. Košnik, Phys. Rev. D **92** (2015) no.1, 014016 [arXiv:1503.09024 [hep-ph]].
 - [15] P. Cox, A. Kusenko, O. Sumensari and T. T. Yanagida, JHEP **1703**, 035 (2017) [arXiv:1612.03923 [hep-ph]].
 - [16] G. Hiller, D. Loose and K. Schönwald, JHEP **1612** (2016) 027 [arXiv:1609.08895 [hep-ph]].
 - [17] G. Hiller and M. Schmaltz, JHEP **1502** (2015) 055 [arXiv:1411.4773 [hep-ph]].
 - [18] W. Altmannshofer, P. Stangl and D. M. Straub, Phys. Rev. D **96**, no. 5, 055008 (2017) [arXiv:1704.05435 [hep-ph]].
 - [19] G. D’Amico, M. Nardecchia, P. Panci, F. Sannino, A. Strumia, R. Torre and A. Urbano, JHEP **1709**, 010 (2017) [arXiv:1704.05438 [hep-ph]].
 - [20] B. Capdevila, A. Crivellin, S. Descotes-Genon, J. Matias and J. Virto, arXiv:1704.05340 [hep-ph].
 - [21] G. Hiller and I. Nišandžić, Phys. Rev. D **96**, no. 3, 035003 (2017) [arXiv:1704.05444 [hep-ph]].

- [22] L. S. Geng, B. Grinstein, S. Jäger, J. Martin Camalich, X. L. Ren and R. X. Shi, arXiv:1704.05446 [hep-ph].
- [23] M. Ciuchini, A. M. Coutinho, M. Fedele, E. Franco, A. Paul, L. Silvestrini and M. Valli, Eur. Phys. J. C **77**, no. 10, 688 (2017) doi:10.1140/epjc/s10052-017-5270-2 [arXiv:1704.05447 [hep-ph]].
- [24] V. Shiltsev, arXiv:1705.02011 [physics.acc-ph].
- [25] G. Aad *et al.* [ATLAS Collaboration], Eur. Phys. J. C **76**, no. 1, 5 (2016) doi:10.1140/epjc/s10052-015-3823-9 [arXiv:1508.04735 [hep-ex]].
- [26] M. Aaboud *et al.* [ATLAS Collaboration], New J. Phys. **18**, no. 9, 093016 (2016) [arXiv:1605.06035 [hep-ex]].
- [27] V. Khachatryan *et al.* [CMS Collaboration], Phys. Rev. D **93**, no. 3, 032004 (2016) [arXiv:1509.03744 [hep-ex]].
- [28] V. Khachatryan *et al.* [CMS Collaboration], Phys. Rev. D **93** (2016) no.3, 032005 Erratum: [Phys. Rev. D **95** (2017) no.3, 039906] [arXiv:1509.03750 [hep-ex]].
- [29] B. Diaz, M. Schmaltz and Y. M. Zhong, JHEP **1710**, 097 (2017) [arXiv:1706.05033 [hep-ph]].
- [30] M. Mangano, CERN Yellow Report CERN 2017-003-M [arXiv:1710.06353 [hep-ph]].
- [31] U. K. Dey, D. Kar, M. Mitra, M. Spannowsky and A. C. Vincent, arXiv:1709.02009 [hep-ph].
- [32] D. Buttazzo, A. Greljo, G. Isidori and D. Marzocca, arXiv:1706.07808 [hep-ph].
- [33] B. C. Allanach, B. Gripaios and T. You, arXiv:1710.06363 [hep-ph].
- [34] A. Alloul, N. D. Christensen, C. Degrande, C. Duhr and B. Fuks, Comput. Phys. Commun. **185** (2014) 2250 [arXiv:1310.1921 [hep-ph]].
- [35] C. Degrande, C. Duhr, B. Fuks, D. Grellscheid, O. Mattelaer and T. Reiter, Comput. Phys. Commun. **183** (2012) 1201 [arXiv:1108.2040 [hep-ph]].
- [36] J. Alwall *et al.*, JHEP **1407** (2014) 079 [arXiv:1405.0301 [hep-ph]].
- [37] P. H. Chankowski, K. Kowalska, S. Lavignac and S. Pokorski, Phys. Rev. D **71**, 055004 (2005) [hep-ph/0501071].
- [38] C. D. Froggatt and H. B. Nielsen, Nucl. Phys. B **147**, 277 (1979).
- [39] S. Descotes-Genon, L. Hofer, J. Matias and J. Virto, JHEP **1606** (2016) 092 [arXiv:1510.04239 [hep-ph]].
T. Hurth, F. Mahmoudi and S. Neshatpour, JHEP **1412** (2014) 053 [arXiv:1410.4545 [hep-ph]].
W. Altmannshofer and D. M. Straub, Eur. Phys. J. C **75** (2015) no.8, 382 [arXiv:1411.3161 [hep-ph]].
F. Beaujean, C. Bobeth and D. van Dyk, Eur. Phys. J. C **74** (2014) 2897 Erratum: [Eur. Phys. J. C **74** (2014) 3179] [arXiv:1310.2478 [hep-ph]].
- [40] A. Greljo and D. Marzocca, Eur. Phys. J. C **77**, no. 8, 548 (2017) [arXiv:1704.09015 [hep-ph]].
- [41] A. Bessaa and S. Davidson, Eur. Phys. J. C **75**, no. 2, 97 (2015) [arXiv:1409.2372 [hep-ph]].
- [42] L. Di Luzio, M. Kirk and A. Lenz, arXiv:1712.06572 [hep-ph].
- [43] A. Buckley, J. Ferrando, S. Lloyd, K. Nordström, B. Page, M. Rüfenacht, M. Schönherr and G. Watt, Eur. Phys. J. C **75**, 132 (2015) [arXiv:1412.7420 [hep-ph]].
- [44] T. Sjöstrand *et al.*, Comput. Phys. Commun. **191** (2015) 159 [arXiv:1410.3012 [hep-ph]].

- [45] J. de Favereau *et al.* [DELPHES 3 Collaboration], JHEP **1402** (2014) 057 [arXiv:1307.6346 [hep-ex]].
- [46] J. B. Hammett and D. A. Ross, JHEP **1507**, 148 (2015) [arXiv:1501.06719 [hep-ph]].
- [47] E. Conte, B. Fuks and G. Serret, Comput. Phys. Commun. **184** (2013) 222 [arXiv:1206.1599 [hep-ph]].
- [48] G. Cowan, K. Cranmer, E. Gross and O. Vitells, Eur. Phys. J. C **71** (2011) 1554 Erratum: [Eur. Phys. J. C **73** (2013) 2501] [arXiv:1007.1727 [physics.data-an]].
- [49] A. M. Baldini *et al.*, arXiv:1301.7225 [physics.ins-det].
- [50] S. Wehle *et al.* [Belle Collaboration], Phys. Rev. Lett. **118**, no. 11, 111801 (2017) [arXiv:1612.05014 [hep-ex]].
- [51] I. Doršner and A. Greljo, arXiv:1801.07641 [hep-ph].